

Stress and Deformation Analysis of Rotating Thick Truncated Conical Shells of Exponential FGM

*Amit Kumar Thawait**

Department of Mechanical Engineering, Shri Shankaracharya Technical Campus, SSGI Bhilai, Junwani Bhilai, Chhattisgarh, India

Abstract

The present study reports stress and deformation analysis of rotating thick truncated conical shells made of exponentially varying functionally graded material, subjected to linearly varying internal pressure. Material properties of the shells are graded exponentially along the axial direction. Metal-ceramic as well as ceramic-metal (FGM) of aluminum metal and zirconia ceramic is considered. The stresses and deformation behavior are evaluated at different surfaces along the radius and at different angular velocities. A comparison of behavior of FGM shells and homogeneous shell is also made. Numerical results obtained shows that the stresses and deformation are maximum at inner surface, near the bottom zone and it is observed that the effect of angular velocity is more dominant over internal pressure, at high speeds.

Keywords: Thick truncated conical shell, Functionally graded material, Linear elastic analysis, Linear varying pressure

***Author for Correspondence** E-mail: amkthawait@gmail.com

INTRODUCTION

Functionally graded materials (FGMs) are multiphase composite materials that have continuous and smooth spatial variations of physical and mechanical properties. The gradation of material properties in FGMs is achieved by continuously varying the volume fractions of the constituents.

Functionally graded conical shells are widely used in space vehicles, aircrafts, nuclear power plants and many other engineering applications [1]. A semi analytical approach using first-order shear deformation theory (FSDT), Matched asymptotic method (MAM) and multilayer method (MLM), can be adopted for the purpose of elastic analysis of rotating thick truncated conical shells made of functionally graded materials (FGMs) [1–3]. To obtain the elastic behavior of functionally graded thick truncated cone by finite element method, Rayleigh–Ritz energy formulation is applied in [4].

To analyze conical shell problem, a thin shell model was developed by using the modified couple stress theory and the equations of motion are derived with partial differentials

and classical and nonclassical boundary conditions by using Hamilton's principle [5]. The generalized coupled thermoelasticity, based on the Lord–Shulman (L-S) theory was employed to study the transient thermoelastic behavior of rotating functionally graded (FG) truncated conical shells subjected to thermal shock with different boundary conditions in [6]. The stability behavior of functionally graded (FG) truncated conical shell, interacting with two-parameter elastic foundation is investigated within the shear deformation theory (SDT) according to the framework of the Donnell's shell theory [7].

The buckling of freely-supported functionally graded (FG) truncated and complete conical shells under external pressures can be studied in the framework of the shear deformation theory (SDT) [8]. An improved high-order theory can be adopted for temperature-dependent buckling analysis of sandwich conical shell with thin functionally graded (FG) facesheets and homogenous soft core [9]. A free and forced vibration analysis of coupled conical–cylindrical shells with arbitrary boundary conditions is analyzed using a modified Fourier–Ritz method [10]. The

dynamic behavior of functionally graded (FG) truncated conical shells subjected to asymmetric internal ring-shaped moving loads can be obtained by the first-order shear deformation theory (FSDT) using Hamilton's principle, assuming that the material properties have continuous variations in the shell thickness direction [11].

Literature review, although points towards the popularity of the area of investigation of truncated conical shells stress and deformation behavior, however, to the best of the researcher's knowledge, no study has been carried out to date on exponential FGM rotating conical shell.

In the present study, rotating truncated conical shells, made of axially varying FGM whose properties vary exponentially in axial direction are analyzed. Aluminum as a metal and zirconia as ceramic is used and metal-ceramic as well as ceramic-metal FGM shells are considered. The shells are subjected to linearly varying pressure fields at its inner surface having clamped-clamped boundary condition. The work aims at investigating stress and deformation behavior of the shells at different angular velocities and for different homogeneous and FGM material.

MATHEMATICAL FORMULATION

Figure 1 shows the geometric parameters for the modeling of axisymmetric cross section of the truncated conical shell. L and h are length and thickness; and a and b are the inner radius at bottom and top surfaces of the shell. z is the distance of any point within the cross section from central plane, along the radial direction and x is height from the bottom edge, along axial direction. R is the distance of the central plane of the cross section, along the radial direction from the central axis of the shell, which is given by [1]:

$$R = a + \frac{h}{2} - (\tan \beta)x \tag{1}$$

where, β is half of the tapering angle, given as:

$$\beta = \tan^{-1} \left(\frac{a-b}{L} \right) \tag{2}$$

Young's modulus and density of the shell are assumed to vary according to the exponential law (Eqs. 3–6) [12].

$$E(x) = E_A e^{\alpha x} \tag{3}$$

$$\rho(x) = \rho_A e^{\gamma x} \tag{4}$$

$$\alpha = \frac{1}{L} \ln \left(\frac{E_A}{E_B} \right) \tag{5}$$

$$\gamma = \frac{1}{L} \ln \left(\frac{\rho_A}{\rho_B} \right) \tag{6}$$

$E(x)$ and $\rho(x)$ are modulus of elasticity and density at height x ; E_A , E_B and ρ_A , ρ_B are modulus of elasticity and density at the bottom and top surfaces, respectively. Figure 2 shows the boundary conditions applied on the shells. Linearly varying pressure field at the inner surface is given by [1]:

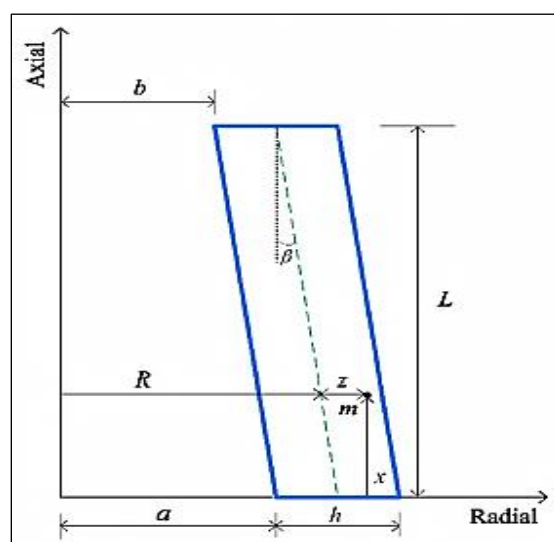


Fig. 1: Geometric Parameters of the Shell.

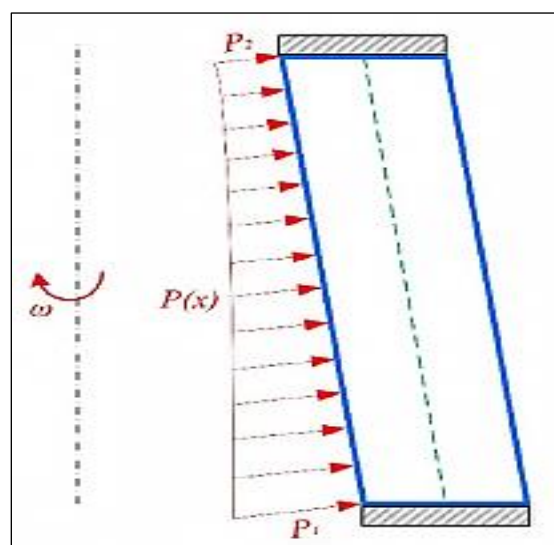


Fig. 2: Boundary Conditions Applied.

$$P(x) = P_1 + (P_2 - P_1) \left(\frac{x}{L} \right) \quad (7)$$

where, P_1 and P_2 are pressure at $x = 0$ and $x = L$. Axial component P_x and radial component P_z of $P(x)$ is given by

$$P_x = P \sin \beta, \quad P_z = P \cos \beta \quad (8)$$

The rotating shell is modeled as an axisymmetric problem. Using quadratic quadrilateral element, the displacement vector $\{\phi\}$ can be obtained as [13]:

$$\{\phi\} = \{u \quad v\}^T = [N] \{\delta\}^e \quad (9)$$

where, u and v are the components of displacement in radial and axial direction, respectively. $[N]$ is the matrix of quadratic shape functions and $\{\delta\}^e$ is the nodal displacement vector, given as:

$$[N] = \begin{bmatrix} N_1 & 0 & N_2 & 0 & \dots & N_8 & 0 \\ 0 & N_1 & 0 & N_2 & \dots & 0 & N_8 \end{bmatrix}$$

$$\{\delta\}^e = \{u_1 \quad v_1 \quad u_2 \quad v_2 \quad \dots \quad u_8 \quad v_8\}^T$$

by transforming the global co-ordinates into natural co-ordinates (ξ - η), the shape functions are obtained as:

$$N_1 = \left(\frac{1}{4} \right) (1 - \xi)(1 - \eta)(-1 - \xi - \eta)$$

$$N_2 = \left(\frac{1}{4} \right) (1 + \xi)(1 - \eta)(-1 + \xi - \eta)$$

$$N_3 = \left(\frac{1}{4} \right) (1 + \xi)(1 + \eta)(-1 + \xi + \eta)$$

$$N_4 = \left(\frac{1}{4} \right) (1 - \xi)(1 + \eta)(-1 - \xi + \eta)$$

$$N_5 = \left(\frac{1}{2} \right) (1 - \xi^2)(1 - \eta)$$

$$N_6 = \left(\frac{1}{2} \right) (1 + \xi)(1 - \eta^2)$$

$$N_7 = \left(\frac{1}{2} \right) (1 - \xi^2)(1 + \eta)$$

$$N_8 = \left(\frac{1}{2} \right) (1 - \xi)(1 - \eta^2)$$

The strain components are related to elemental displacement components by Eqs. (10) to (14), where ϵ_r , ϵ_θ , ϵ_z and γ_{rz} are radial, tangential, axial and shear strain, respectively.

$$\{\epsilon\} = \{\epsilon_r \quad \epsilon_\theta \quad \epsilon_z \quad \gamma_{rz}\}^T = \left\{ \frac{\partial u}{\partial r} \quad \frac{u}{r} \quad \frac{\partial v}{\partial z} \quad \frac{\partial u}{\partial z} + \frac{\partial v}{\partial r} \right\}^T \quad (10)$$

$$\left\{ \frac{\partial u}{\partial r} \quad \frac{u}{r} \quad \frac{\partial v}{\partial z} \quad \frac{\partial u}{\partial z} + \frac{\partial v}{\partial r} \right\}^T = [B_1] \times \left\{ \frac{\partial u}{\partial r} \quad \frac{\partial u}{\partial z} \quad \frac{\partial v}{\partial r} \quad \frac{\partial v}{\partial z} \quad \frac{u}{r} \right\}^T \quad (11)$$

By transforming the global co-ordinates into natural co-ordinates (ξ - η),

$$\left\{ \frac{\partial u}{\partial r} \quad \frac{\partial u}{\partial z} \quad \frac{\partial v}{\partial r} \quad \frac{\partial v}{\partial z} \quad \frac{u}{r} \right\}^T = [B_2] \times \left\{ \frac{\partial u}{\partial \xi} \quad \frac{\partial u}{\partial \eta} \quad \frac{\partial v}{\partial \xi} \quad \frac{\partial v}{\partial \eta} \quad \frac{u}{r} \right\}^T \quad (12)$$

$$\left\{ \frac{\partial u}{\partial \xi} \quad \frac{\partial u}{\partial \eta} \quad \frac{\partial v}{\partial \xi} \quad \frac{\partial v}{\partial \eta} \quad \frac{u}{r} \right\}^T = [B_3] \times \{\delta\}^e \quad (13)$$

The above elemental strain-displacement relationships can be written as:

$$\{\varepsilon\} = [B] \{\delta\}^e \quad (14)$$

where, $[B]$ is strain-displacement relationship matrix, which contains derivatives of shape functions.

For a quadratic quadrilateral element it is calculated as:

$$[B] = [B_1] \times [B_2] \times [B_3] \quad (15)$$

$$[B_1] = \begin{bmatrix} 1 & 0 & 0 & 0 & 0 \\ 0 & 0 & 0 & 0 & 1 \\ 0 & 0 & 0 & 1 & 0 \\ 0 & 1 & 1 & 0 & 0 \end{bmatrix} \quad (16)$$

$$[B_2] = \begin{bmatrix} \frac{J_{22}}{|J|} & \frac{-J_{12}}{|J|} & 0 & 0 & 0 \\ \frac{-J_{21}}{|J|} & \frac{J_{11}}{|J|} & 0 & 0 & 0 \\ 0 & 0 & \frac{J_{22}}{|J|} & \frac{-J_{12}}{|J|} & 0 \\ 0 & 0 & \frac{-J_{21}}{|J|} & \frac{J_{11}}{|J|} & 0 \\ 0 & 0 & 0 & 0 & 1 \end{bmatrix} \quad (17)$$

where, J is the Jacobian matrix, used to transform the global co-ordinates into natural co-ordinates. It is given as:

$$[J] = \begin{bmatrix} \sum_{i=1}^8 \frac{\partial N_i}{\partial \xi} r_i & \sum_{i=1}^8 \frac{\partial N_i}{\partial \xi} z_i \\ \sum_{i=1}^8 \frac{\partial N_i}{\partial \eta} r_i & \sum_{i=1}^8 \frac{\partial N_i}{\partial \eta} z_i \end{bmatrix} \quad (18)$$

$$[B_3] = \begin{bmatrix} \frac{\partial N_1}{\partial \xi} & 0 & \frac{\partial N_2}{\partial \xi} & 0 & \frac{\partial N_3}{\partial \xi} & 0 & \frac{\partial N_4}{\partial \xi} & 0 \\ \frac{\partial N_1}{\partial \eta} & 0 & \frac{\partial N_2}{\partial \eta} & 0 & \frac{\partial N_3}{\partial \eta} & 0 & \frac{\partial N_4}{\partial \eta} & 0 \\ 0 & \frac{\partial N_1}{\partial \xi} & 0 & \frac{\partial N_2}{\partial \xi} & 0 & \frac{\partial N_3}{\partial \xi} & 0 & \frac{\partial N_4}{\partial \xi} \\ 0 & \frac{\partial N_1}{\partial \eta} & 0 & \frac{\partial N_2}{\partial \eta} & 0 & \frac{\partial N_3}{\partial \eta} & 0 & \frac{\partial N_4}{\partial \eta} \\ \frac{N_1}{r} & 0 & \frac{N_2}{r} & 0 & \frac{N_3}{r} & 0 & \frac{N_4}{r} & 0 \end{bmatrix} \quad (19)$$

From generalized hooks law, components of stresses in radial, circumferential and axial direction (σ_r , σ_θ , σ_z and τ_{rz}) are related to components of total strain as:

$$\varepsilon_r = \frac{1}{E}(\sigma_r - \nu\sigma_\theta - \nu\sigma_z) \quad (20)$$

$$\varepsilon_\theta = \frac{1}{E}(\sigma_\theta - \nu\sigma_r - \nu\sigma_z) \quad (21)$$

$$\varepsilon_z = \frac{1}{E}(\sigma_z - \nu\sigma_\theta - \nu\sigma_r) \quad (22)$$

In generalized matrix notation, stress-strain relation can be written as:

$$\{\sigma\} = [D(x)]\{\varepsilon\} \quad (23)$$

$$\{\sigma\} = \{\sigma_r \quad \sigma_\theta \quad \sigma_z \quad \tau_{rz}\}^T \quad (24)$$

$$D(x) = \frac{(1-\nu)E(x)}{(1+\nu)(1-2\nu)} \begin{bmatrix} 1 & \frac{\nu}{(1-\nu)} & \frac{\nu}{(1-\nu)} & 0 \\ \frac{\nu}{(1-\nu)} & 1 & \frac{\nu}{(1-\nu)} & 0 \\ \frac{\nu}{(1-\nu)} & \frac{\nu}{(1-\nu)} & 1 & 0 \\ 0 & 0 & 0 & \frac{1-2\nu}{2(1-\nu)} \end{bmatrix} \quad (25)$$

$$\{\varepsilon\} = \{\varepsilon_r \quad \varepsilon_\theta \quad \varepsilon_z \quad \gamma_{rz}\}^T \quad (26)$$

When the shell rotates and is subjected to internal pressure, it experiences a distributed force over its volume and surface. Under these forces when shell is properly supported (so as to prevent rigid body motion), it undergoes deformation and stores internal strain energy U , which is given by Eq. (27).

$$U = \frac{1}{2} \int_V \{\varepsilon\}^T \{\sigma\} dv \quad (27)$$

Also the potential of external body and surface force is given by

$$V = - \int_V \{\delta\}^T \{q_v\} dv - \int_S \{\delta\}^T \{q_s\} ds \quad (28)$$

The element level equation can be written as

$$U^e = \int_V \frac{1}{2} \{\delta\}^{eT} [B]^T [D(r)] [B] \{\delta\}^e dv \quad (29)$$

$$V^e = - \int_V \{\delta\}^{eT} [N]^T \{q_v\} dv - \int_S \{\delta\}^{eT} [N]^T \{q_s\} ds \quad (30)$$

The total potential of the element can be written as

$$\pi_p^e = \int_V \frac{1}{2} \{\delta\}^{eT} [B]^T [D(r)] [B] \{\delta\}^e dv - \int_V \{\delta\}^{eT} [N]^T \{q_v\} dv - \int_S \{\delta\}^{eT} [N]^T \{q_s\} ds \quad (31)$$

Defining element stiffness matrix $[K]^e$ and element load vector $\{f\}^e$ as:

$$[K]^e = \int_V [B]^T [D(r)] [B] dv \tag{32}$$

$$\{f\}^e = \int_V [N]^T \{q_v\} dv + \int_S [N]^T \{q_s\} ds \tag{33}$$

Taking axisymmetric element, thickness of the element will be $2\pi r$, therefore:

$$[K]^e = 2\pi \int \int [B]^T [D(r)] [B] r dr dz \tag{34}$$

$$\{f\}^e = 2\pi \int_V [N]^T \{q_v\} r dr dz + \int_S [N]^T \{q_s\} r dr dz \tag{35}$$

Transforming global co-ordinates into natural co-ordinates

$$[K]^e = 2\pi \int_{-1}^1 \int_{-1}^1 [B]^T [D(r)] [B] r |J| d\xi d\eta \tag{36}$$

$$\{f\}^e = 2\pi \int_V [N]^T \{q_v\} r |J| d\xi d\eta + \int_S [N]^T \{q_s\} |J| d\xi d\eta \tag{37}$$

where J is the Jacobian matrix, which is given by Eq. (18).

Total potential energy of the shell is given by

$$\pi_p = \sum \pi_p^e \tag{38}$$

Using the Principle of stationary total potential (PSTP) the total potential is set to be stationary with respect to small variation in the nodal degree of freedom that is:

$$\frac{\partial \pi_p}{\partial \{\delta\}^T} = 0 \tag{39}$$

which gives system level equation for shell as:

$$[K] \{\delta\} = \{F\} \tag{40}$$

Where

$$[K] = \sum_{n=1}^N [K]^e = \text{Global Stiffness matrix}$$

$$\{F\} = \sum_{n=1}^N \{f\}^e = \text{Global load vector}$$

RESULTS AND DISCUSSION

Validation of the Work

To validate the current research work, a similar system of conical shell which is previously analyzed is reconsidered. The shell has geometric parameters [1] as: $L = 400$ mm, $h = 20$ mm, $a = 40$ mm and $b = 30$ mm. Material gradation is done by power law, and shell has clamped-clamped boundary condition. Circumferential stresses for $\omega = 0, 1000$ and 2000 rad/s are evaluated taking $m = n = 1$ and a comparison with reference is presented in Figure 3. Both the results are in good agreement.

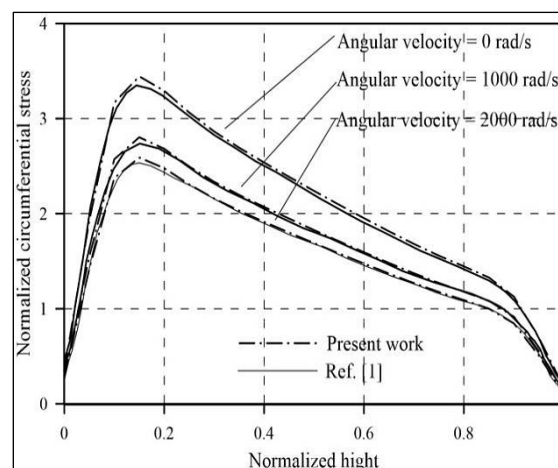


Fig. 3: Validation of the Work.

Numerical Results

In this section a conical shell made up of exponentially varying FGM is analyzed. Aluminum as metal and zirconia as ceramic is taken and Ceramic-metal and Metal-ceramic both the FGM shell is analyzed. The material properties of aluminum and zirconia are given as [14]:

$$E_{Al} = 70 \text{ GPa}, E_{cer} = 151 \text{ GPa}, \rho_{Al} = 2700 \text{ kg/m}^3, \rho_{cer} = 5700 \text{ kg/m}^3,$$

The shell has same geometric parameters as discussed above [1], that is $L = 400 \text{ mm}$, $h = 20 \text{ mm}$, $a = 40 \text{ mm}$ and $b = 30 \text{ mm}$. Shell has clamped-clamped boundary condition. P_1 and P_2 are taken as 120 MPa and 40 MPa .

Figures 4 to 7 show the distributions of normalized radial displacement, radial stress, circumferential stress and shear stress, respectively. All the distributions are along the axial direction and evaluated at 1000 rad/s , for metal-ceramic FGM shells. It is observed that deformation in radial direction is minimum that is zero at bottom and top surface, which confirms the clamped-clamped boundary condition applied to the shell. Deformations are maximum at the inner layer, i.e., at $z = -h/2$ and decreases gradually till the outer layer ($z =$

$h/2$). It is maximum near the bottom surface and gradually decreases till the top surface. Radial stresses are tensile and compressive both in nature while circumferential stresses are only tensile. Compressive radial stress is more as compared to tensile radial stress. Tensile radial stress occurs only in a small zone near top and bottom surface and rest of the intermediate height zone has compressive radial stress. Circumferential stress has same distribution pattern as radial displacement. It is maximum at the inner layer, near the bottom surface, and decreases gradually up to the top surface and outer layer. Shear stress varies only in a small zone near the top and bottom surface and remains same in all the layers at intermediate heights. It is maximum at the bottom surface, i.e., at $x = 0$.

It can be seen from Figures 8 and 9. that deformation and stresses both increase with increasing angular velocity but at lower speeds (less than 500 rad/s), the effect of angular velocity is very less, since below this speed, stresses due to internal pressure is more dominant and above this speed, centrifugal force and stress has a significant value as compared to internal pressure.

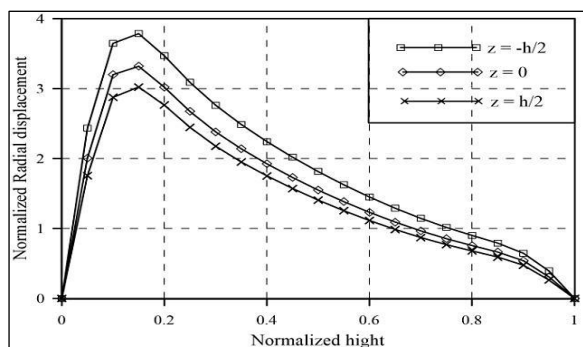


Fig. 4: Normalized Radial Displacement ($\omega = 1000$).

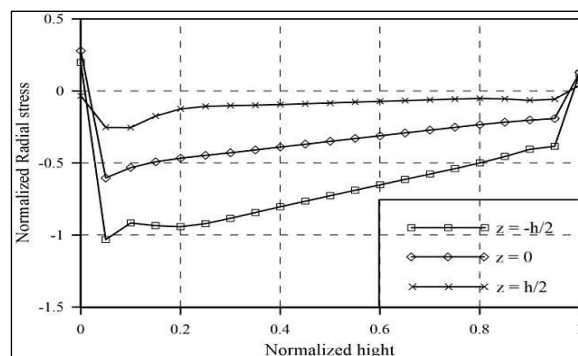


Fig. 5: Normalized Radial Stress ($\omega = 1000$).

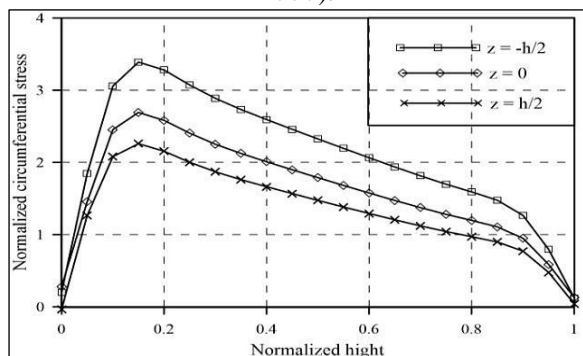


Fig. 6: Normalized Circumferential Stress ($\omega = 1000$).

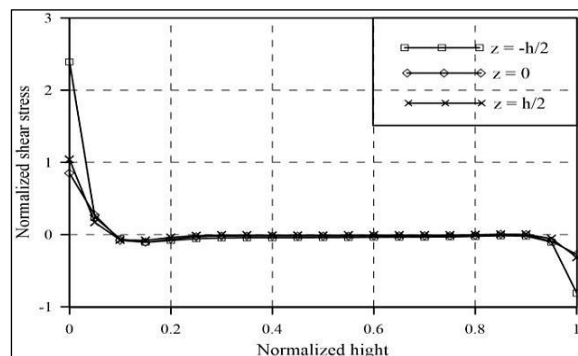


Fig. 7: Normalized Shear Stress ($\omega = 1000$).

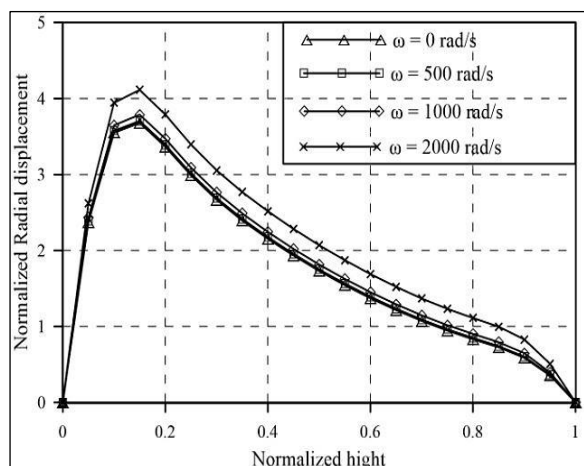


Fig. 8: Normalized Radial Displacement ($z = -h/2$).

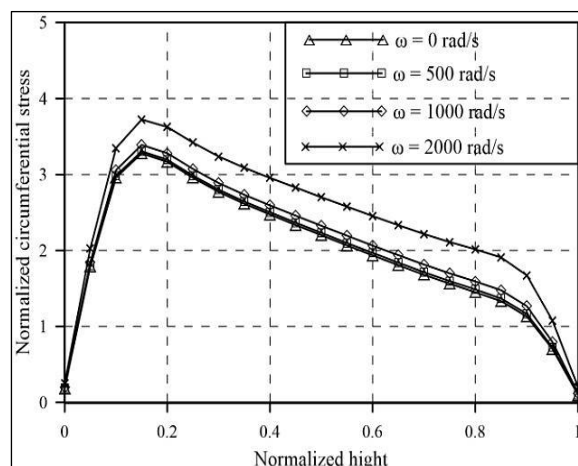


Fig. 9: Normalized Circumferential Stress ($z = -h/2$).

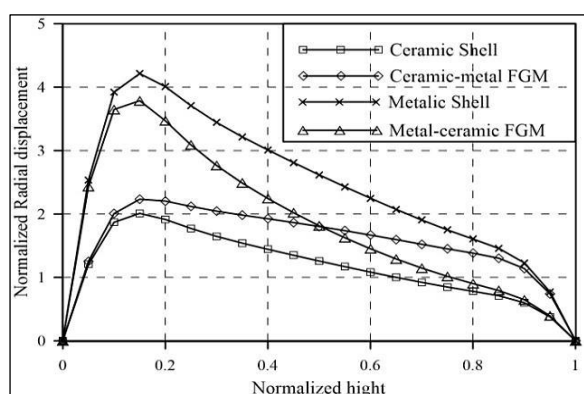


Fig. 10: Normalized Radial Displacement ($z = -h/2$, $\omega = 1000$).

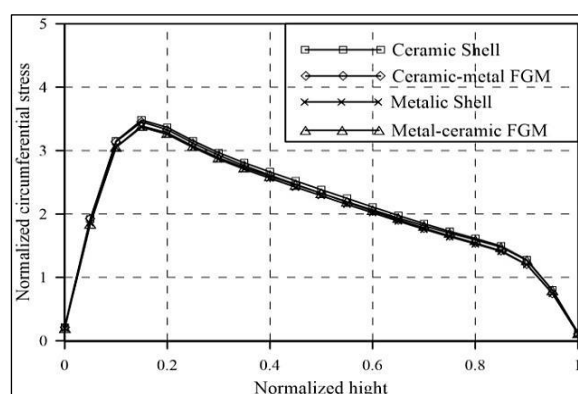


Fig. 11: Normalized Circumferential Stress ($z = -h/2$, $\omega = 1000$).

Figures 10 and 11; show the distribution of radial displacement and circumferential stress for different types of materials. It can be seen that material has a significant role in deformation but has very low effect on stresses. Homogeneous ceramic material shell has minimum radial deformation and homogeneous metallic shell has maximum deformation but at the same time ceramic has highest density and metal has lowest density. Therefore, to optimize deformation to weight ratio, ceramic-metal FGM is best suitable for conical shell structure.

CONCLUSION

In the present study stress and deformation analysis of rotating thick truncated conical shells made up of functionally graded material is done. Material properties are modeled by exponential law which is achieved by element based material grading. The shells are subjected to clamped-clamped boundary condition and linearly varying pressure field at

its inner surface. The governing equations are modeled using principle of stationary total potential. Numerical results are obtained for metal-ceramic and ceramic-metal FGM of aluminum and zirconia. The results obtained are found to be in good agreement with established reports. On the basis of results obtained it can be concluded that deformation and stresses are more in the inner layer, near the bottom surface and increases with increasing angular velocity. The effect of rotation is considerable above 500 rad/s angular velocity. To optimize deformation to weight ratio, ceramic-metal FGM is best suitable for truncated conical shell structure.

REFERENCES

1. Nejad MZ, Jabbari M, Ghannad M. Elastic analysis of FGM rotating thick truncated conical shells with axially-varying properties under non-uniform pressure loading. *Compos Struct.* 2015; 122: 561–569p.

2. Nejad MZ, Jabbari M, Ghannad M. Elastic Analysis of Rotating Thick Truncated Conical Shells Subjected to Uniform Pressure Using Disk Form Multilayers. *ISRN Mech Eng.* 2014; 2014: 1–10p.
3. Nejad MZ, Jabbari M, Ghannad M. A Semi Analytical Solution of Thick Truncated Cones using Matched Asymptotic Method and Disk form Multilayers. *Arch Mech Eng.* 2014; 61: 495–513p.
4. Asemi K, Akhlaghi M, Salehi M, *et al.* Analysis of functionally graded thick truncated cone with finite length under hydrostatic internal pressure. *Arch Appl Mech.* 2011; 81: 1063–1074p.
5. Zeighampour H, Beni YT. Analysis of conical shells in the framework of coupled stresses theory. *Int J Eng Sci.* 2014; 81: 107–122p.
6. Heydarpour Y, Aghdam MM. Transient analysis of rotating functionally graded truncated conical shells based on the Lord–Shulman model. *Thin-Walled Struct.* 2016; 104: 168–184p.
7. Sofiyev AH, Kuruoglu N. Combined effects of elastic foundations and shear stresses on the stability behavior of functionally graded truncated conical shells subjected to uniform external pressures. *Thin-Walled Struct.* 2016; 102: 68–79p.
8. Sofiyev AH. Buckling analysis of freely-supported functionally graded truncated conical shells under external pressures. *Compos Struct.* 2015; 132: 746–758p.
9. Seidi J, Khalili SMR, Malekzadeh K. Temperature-dependent buckling analysis of sandwich truncated conical shells with FG facesheets. *Compos Struct.* 2015; 131: 682–691p.
10. Ma X, Jin G, Xiong Y, *et al.* Free and forced vibration analysis of coupled conical–cylindrical shells with arbitrary boundary conditions. *Int J Mech Sci.* 2014; 88:122–137p.
11. Malekzadeh P, Daraie M. Dynamic analysis of functionally graded truncated conical shells subjected to asymmetric moving loads. *Thin-Walled Struct.* 2014; 84: 1–13p.
12. Afsar AM, Go J. Finite element analysis of thermoelastic field in a rotating FGM circular disk. *Appl Math Modell.* 2010; 34: 3309–3320p.
13. Seshu P. *Two dimensional finite element analysis a text book of finite element analysis.* PHI Learning Pvt. Ltd. 2003; Ch 5: 167–171p.
14. Bayat M, Sahari B, Saleem M, *et al.* Analysis of functionally graded rotating disks with parabolic concave thickness applying an exponential function and the Mori-Tanaka scheme. *IOP Conf. Series: Mater Sci Eng.* 2011; 17: 1–11p.

Cite this Article

Amit Kumar Thawait. Stress and Deformation Analysis of Rotating Thick Truncated Conical Shells of Exponential FGM. *Research & Reviews: Journal of Physics.* 2016; 5(2): 36–44p.